Electronic Supplementary Material (ESI) for Nanoscale.

Blue sensitive sub-band gap negative photoconductance in SnO_2/TiO_2 NPs bilayer oxide transistor

Utkarsh Pandey[a¶], Nila Pal[a¶], Arpan Ghosh[a], Swati Suman[a,b], Sajal Biring*[c] and Bhola N. Pal[a*]

[a]*School of Materials Science and Technology, Indian Institute of Technology (Banaras Hindu University), Varanasi-221005, India,*

[b]*Electronic Materials and Thin Films Lab, Department of Metallurgical and Materials Engineering, Indian Institute of Technology (IIT) Madras, Chennai, India*

[c]*Department of Electronic Engineering, Ming Chi University of Technology, New Taipei City, Taiwan 243*

**Corresponding author E-mail ID: bnpal.mst@iitbhu.ac.in, biring@mail.mcut.edu.tw*

¶ *Those two authors contributed equally.*

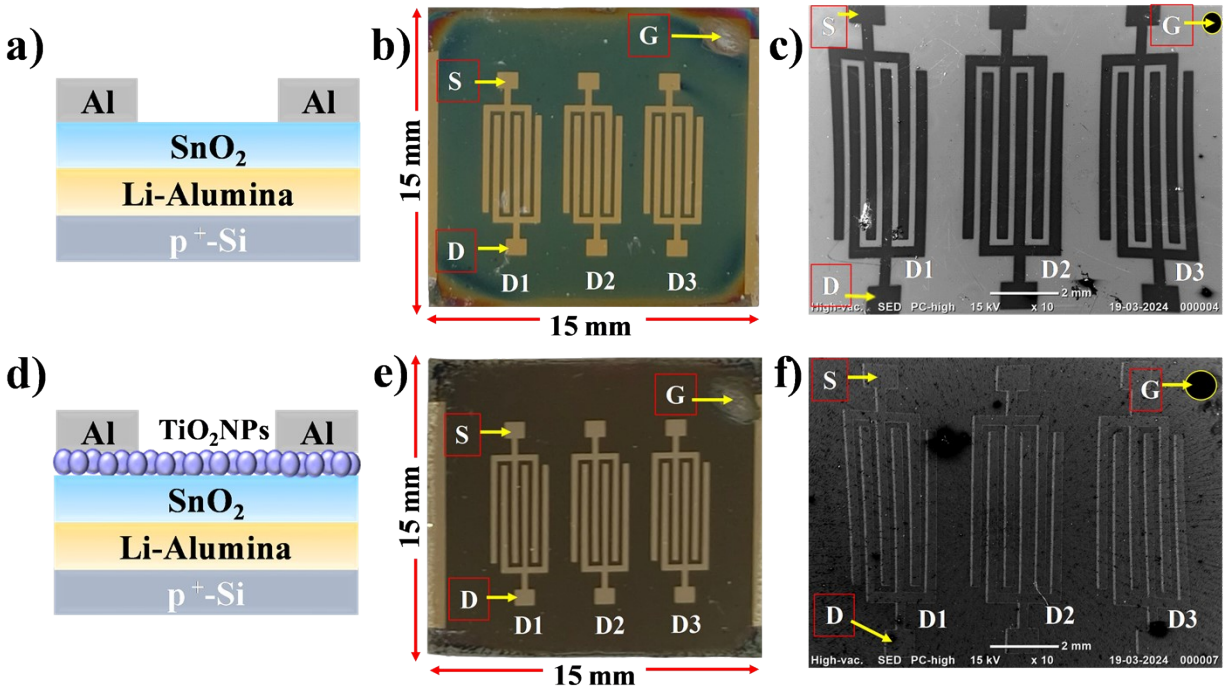

Figure SI 1 The a) schematic diagram b) actual device c) SEM Image of the TFT 1 and d) schematic diagram e) actual device f) SEM Image of the TFT 2.

Structural analysis of SnO_2 and TiO_2 NPs

The structural analysis of SnO_2 in this film and TiO_2 nanoparticles (NPs) was conducted through thin-film X-ray diffraction (XRD) patterns. This experiment involved the examination of drop-cast films of SnO_2 annealed at 500 °C for 30 minutes and TiO_2 NP thin films annealed at 120°C for 60 minutes. In Figure S1, the X-ray diffraction (XRD) pattern of both the SnO_2 and TiO_2 NPs thin film samples is presented, revealing distinct diffraction peaks with noticeable broadening, indicative of the nanocrystalline nature of the particles. Based on this data, the XRD peaks for TiO_2 are situated at 24.19º, 36.75º, 46.90º, and 61.75º, corresponding to the (101), (004), (200), and (211) crystallographic planes[1], respectively (JCPDS, 21-1272). This pattern suggests the presence of the anatase phase in TiO_2. On the other hand, the XRD peaks for SnO_2 are detected at 25.4º, 32.63º, and 50.69º, corresponding to the (211), (101), and (110) crystallographic planes of the tetragonal phase of SnO_2 (JCPDS 88-0287)[2].

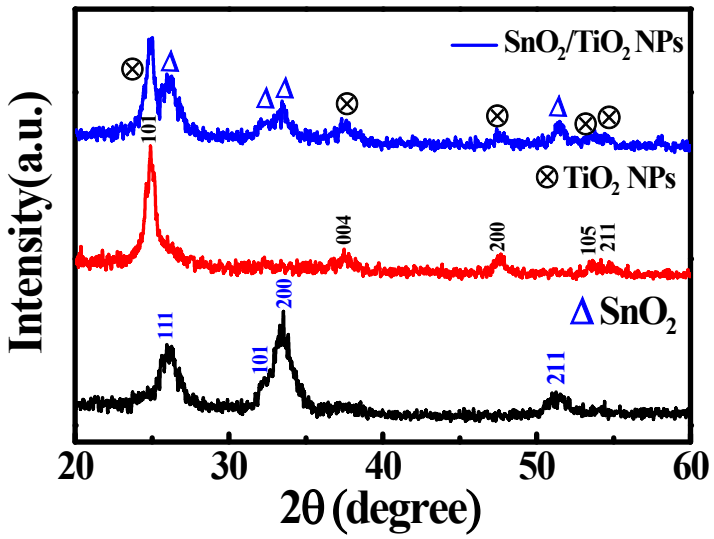

Figure SI 2 XRD pattern of the SnO_2, TiO_2 NPs, and SnO_2/TiO_2 films.

Optical analysis of SnO_2 and TiO_2 NPs films

The UV-Vis absorption data for SnO_2, TiO_2, and the SnO_2/TiO_2 heterojunction thin film are illustrated in Figure SI2 a). In Figure SI2 b), Tauc's plot of the absorption data reveals that both SnO_2 and TiO_2 possess direct band gaps of 3.48 eV and 3.34 eV, respectively. Interestingly, the heterojunction thin film demonstrates a band gap of 3.34 eV. This reveals that the optical property of the SnO_2/TiO_2 hetrostructure is very close to the TiO_2 NPs.

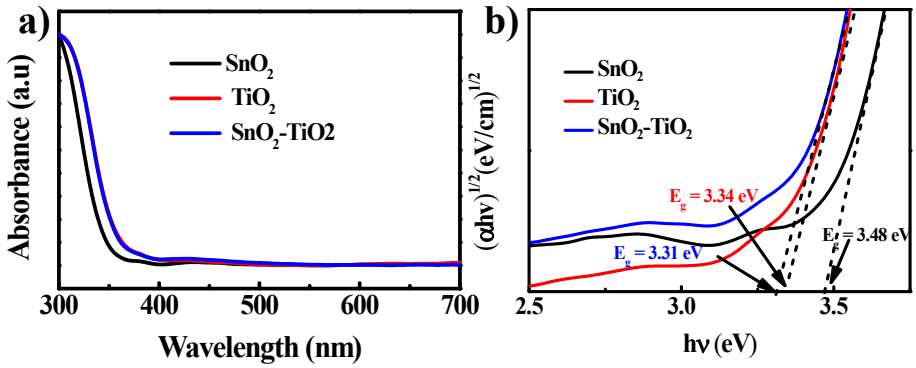

Figure SI 3 UV-Vis (a) absorption spectra of the SnO_2, TiO_2, and SnO_2/TiO_2 heterostructure and (b) Tauc's plot of the absorption data

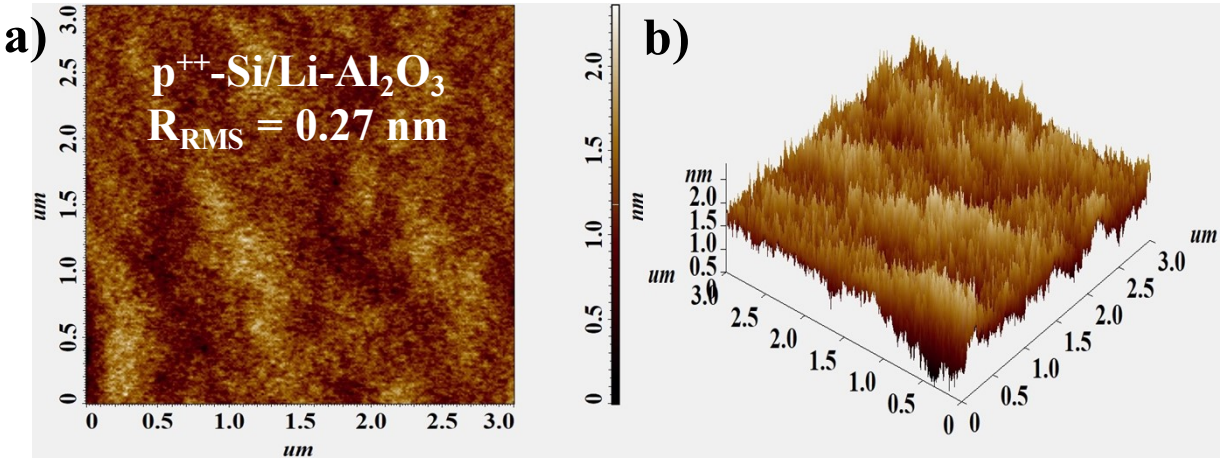

Figure SI 4 Surface morphology of Li-Al_2O_3 dielectric on p^+-Si substrate in a) 2D and b) 3D by atomic force microscopy (AFM).

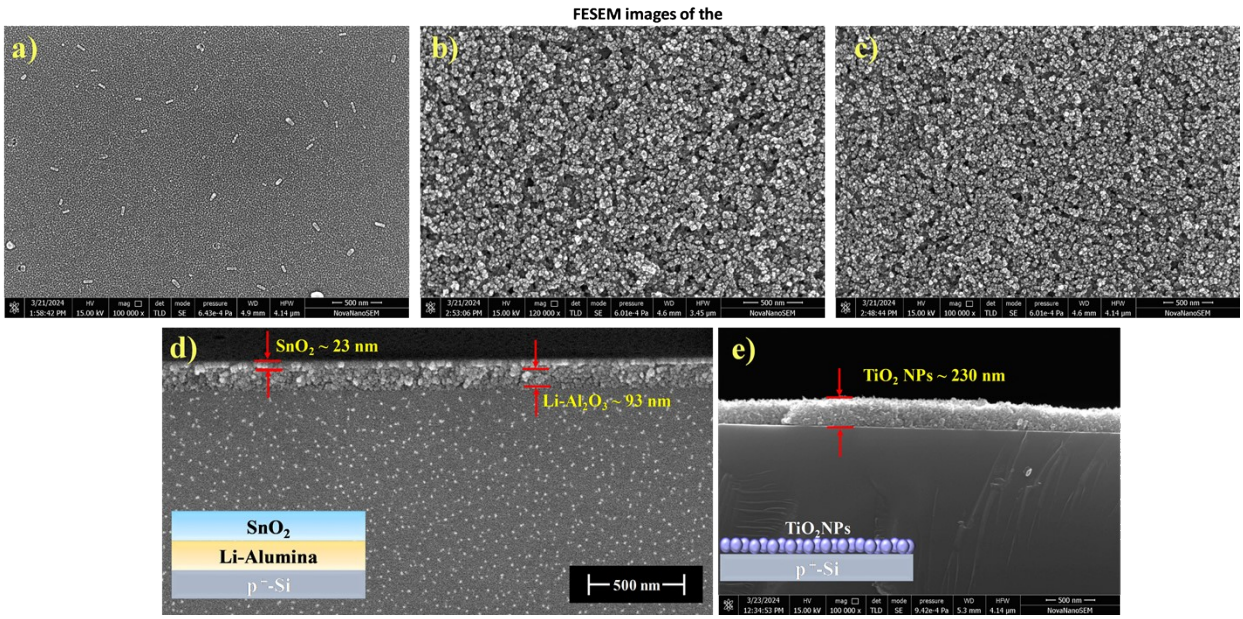

Figure SI 5 The FESEM images of the a) SnO_2, b) TiO_2 and c) SnO_2/TiO_2 NPs; The cross-sectional SEM image of the d) SnO_2/Li-Al_2O_3 bilayer (p^+-Si/Li-Al_2O_3/SnO_2) and e) TiO_2 NPs layer (p^+-Si/TiO_2 NPs).

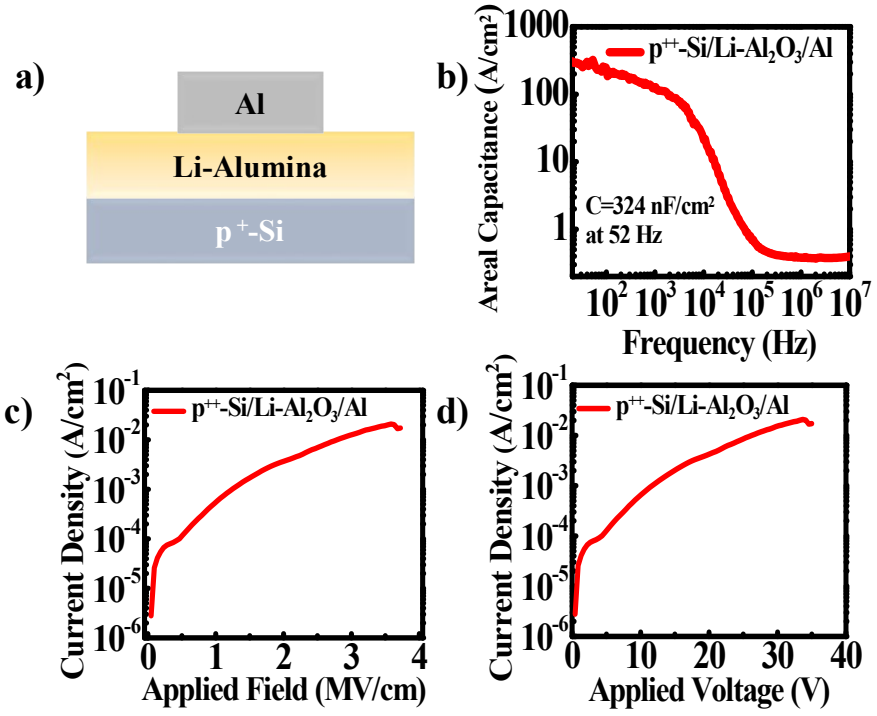

Figure SI 6 Dielectric property measurement of Li-Al_2O_3 a) Schematic diagram of the MIM (p^+-Si/Li-Al_2O_3/Al) configuration, b) Capacitance vs. frequency plot, c) Current density vs. applied field, and d) current density vs. applied voltage.

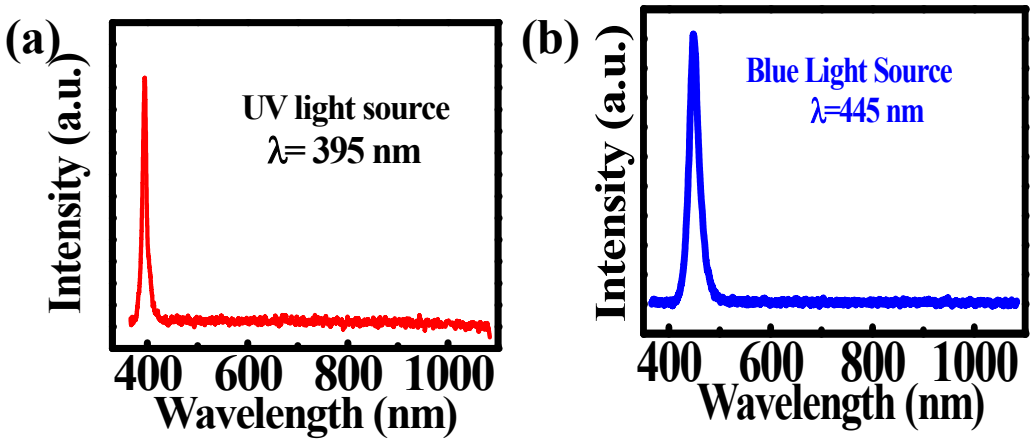

Figure SI 7 Emission spectra of a) UV light source, and b) blue light source

The Optical response of the TFT1

The optical response of the TFT 1 has been tested under two LED light sources (UV and blue) with wavelength 395 and 445 nm has been used to illuminate the devices. The spectra of these light sources have been shown in figure SI 5 a) and b), having peak intensities at wavelengths of 395 and 445 nm, respectively. Figure SI 8 a), shows the optical illumination of the TFT 1 under UV light and the variation of the drain current in transfer and output characteristics under UV illumination for TFT 1 is shown in Figure SI 8 a) and SI 8 b), respectively. Under UV illumination, in both of the characteristics the drain current of the device is increases with UV illumination (direction of black arrow shows). Here, an increase in the photocurrent upon light illumination has been observed, which is feasible with SnO_2 semiconductor because of its wide bandgap, thus UV light-sensitive[43]. This behavior is commonly referred to as the positive photoconductance nature of the device and is particularly pronounced when using optically sensitive materials, such as metal oxide, in TFTs. The working mechanism of the SnO_2 TFT under UV illumination has been

illustrated in Figure SI 8 d). In contrast, the device is not giving any practical change in the transfer characteristics under blue illumination, (Figure SI 8 g&h)).

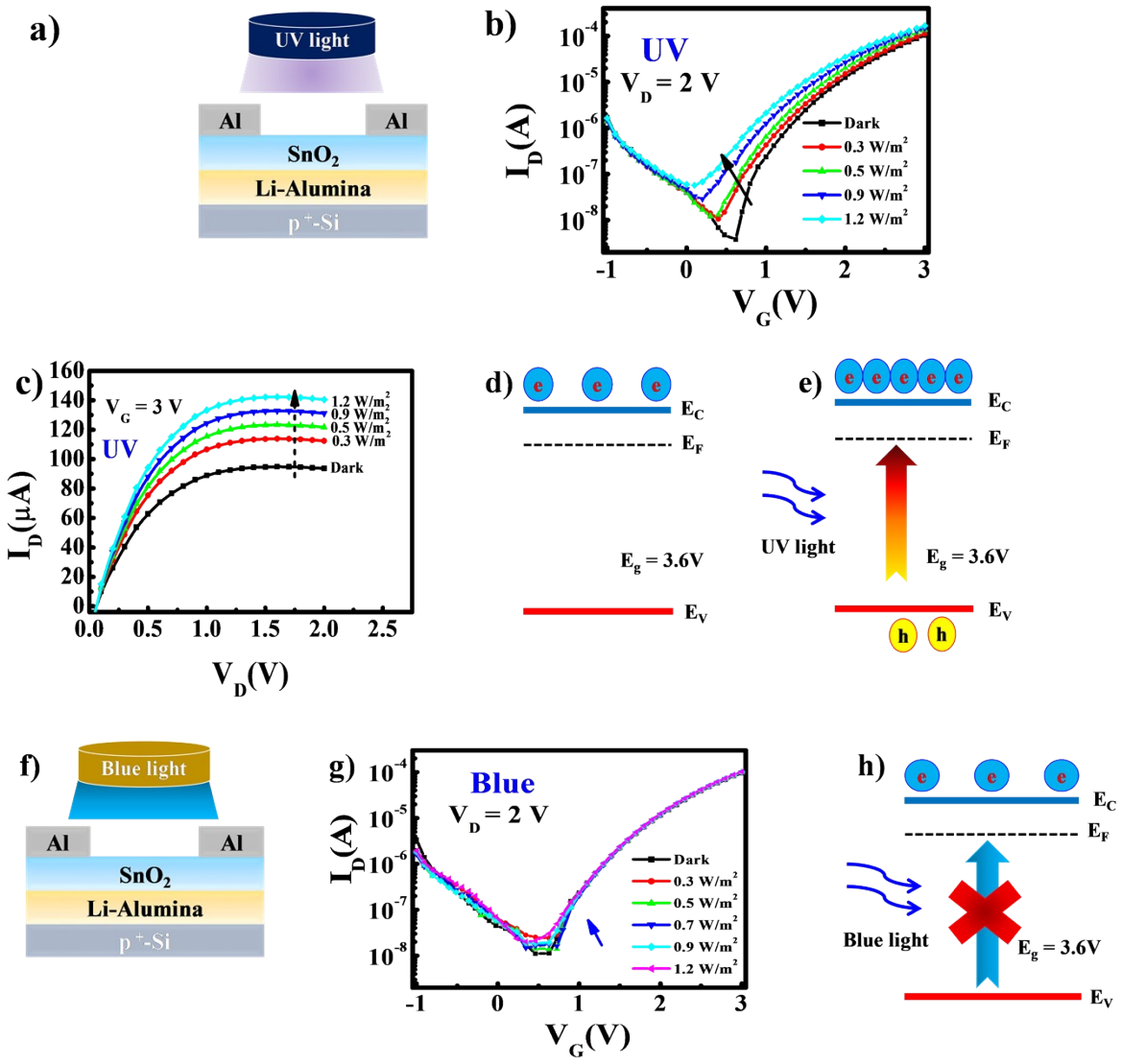

Figure SI 8 a) Schematics of TFT 1 under UV illumination, b) Transfer characteristics at V_D=2V, and c) Output characteristics at V_G = 3 V of the phototransistor with dark and different UV light (λ=395 nm) intensities, black arrow shows the positive shift under UV illumination; d) Schematic diagram of energy band SnO_2 before and after UV illumination; e) Schematic diagram of bare SnO_2 transistor illuminated with blue light source and f) Transfer characteristics of the device under dark and blue light illumination at a constant drain voltage of 2V, g) f) energy band diagram of SnO_2 and failed electron-hole pair generation during blue light illumination.

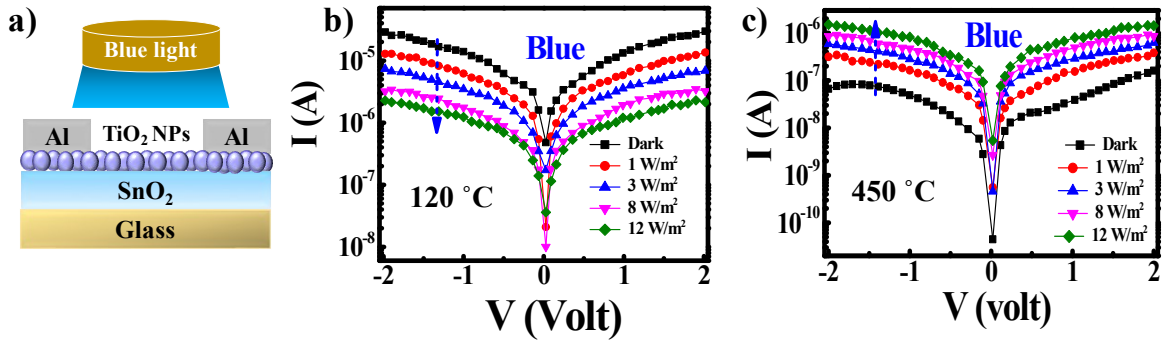

Figure SI 9 a) Schematic diagram of SnO_2/TiO_2 heterostructure based photoconductor andthe I-V plot of SnO_2/TiO_2 heterostructure with b) TiO_2 NPs annealing temperature 120℃ for 1 h (blue arrow shows the direction of photo conductance) showing NPC and c) TiO_2 NPs annealing temperature 450℃ for 1 h (blue arrow shows the direction of photo conductance) showing PPC behavior.

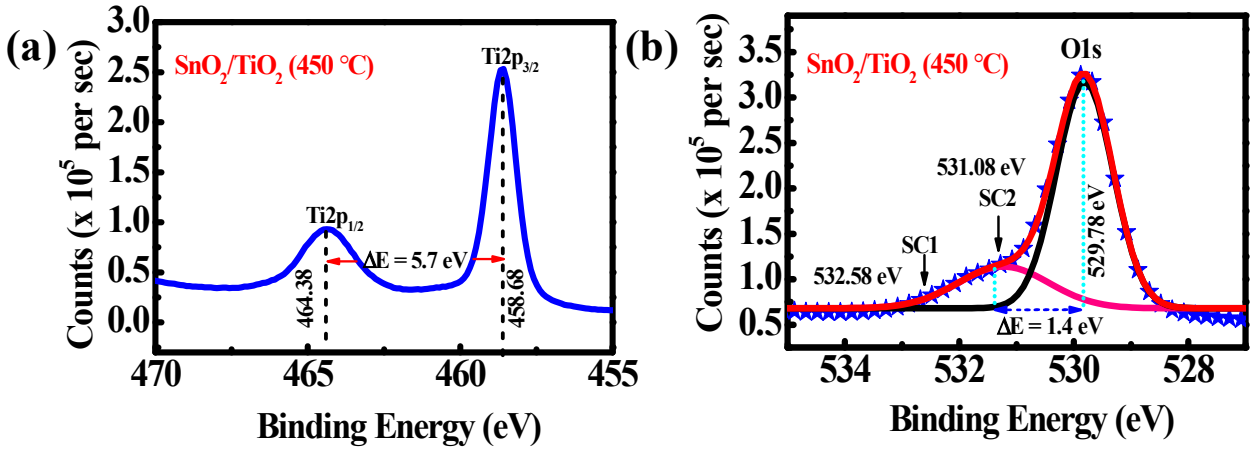

Figure SI 10 The XPS data of the SnO_2/TiO_2 heterostructure film a) Ti2p spectrum b) O1s core spectrum with TiO_2 NPs annealing at 450 °C

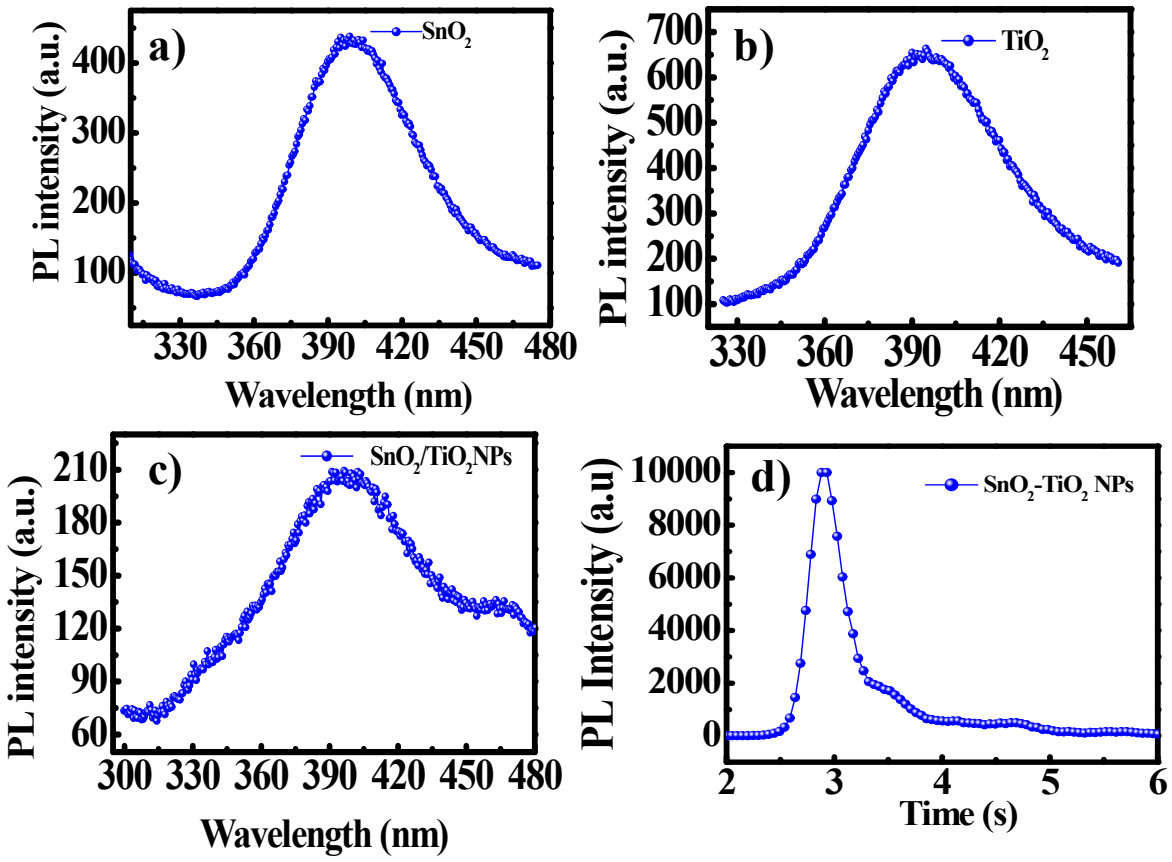

Figure SI 11 The photo photoluminescence (PL) spectra of the a) SnO_2, b) TiO_2 NPs and c) SnO_2/TiO_2 NPs layer; Time resolved PL spectra of SnO_2/TiO_2 NPs layer.

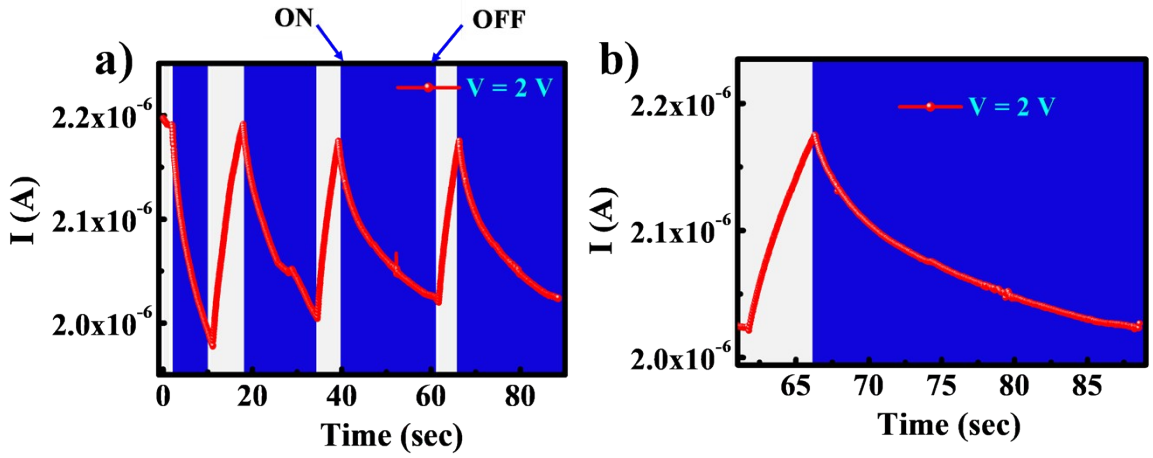

Figure SI 12. The transient response of the TFT 2 for prolonged (more than 20 sec) blue light illumination a) multiple cycle b) single cycle at intensity 1.2 W/m^2.

[1] J. Lin, W. Ren, A. Li, C. Yao, T. Chen, X. Ma, X. Wang, A. Wu, Crystal–amorphous core–shell structure synergistically enabling TiO2 nanoparticles' remarkable SERS sensitivity for cancer cell imaging, ACS applied materials & interfaces 12(4) (2019) 4204-4211.
[2] N. Pal, U. Pandey, S. Biring, B.N. Pal, Solution processed low-voltage metal-oxide transistor by using TiO2/Li–Al2O3 stacked gate dielectric, Journal of Materials Science: Materials in Electronics 33(12) (2022) 9580-9589.